Physicochemical characterization of a lycopene-loaded mesoporous silica nanoparticle formulation

Gabriela Corrêa Carvalho (gabrielacarvalho57@yahoo.com)
School of Pharmaceutical Sciences, São Paulo State University (UNESP), 14800-903 Araraquara, Brazil; Department of Biomedical Engineering, University Medical Center Groningen, University of Groningen Ant. Deusinglaan 1, Groningen 9713 AV, The Netherlands; W.J. Kolff Institute for Biomedical Engineering and Materials Science, University Medical Center Groningen, University of Groningen Ant. Deusinglaan 1, Groningen 9713 AV, The Netherlands

Gabriel Davi Marena
School of Pharmaceutical Sciences, São Paulo State University (UNESP), 14800-903 Araraquara, Brazil

André Luiz Carneiro Soares do Nascimento
School of Pharmaceutical Sciences, São Paulo State University (UNESP), 14800-903 Araraquara, Brazil

Bruna Almeida Furquim Camargo
School of Pharmaceutical Sciences, São Paulo State University (UNESP), 14800-903 Araraquara, Brazil

Rafael Miguel Sábio
School of Pharmaceutical Sciences, São Paulo State University (UNESP), 14800-903 Araraquara, Brazil

Felipe Rebello Lourenço
Faculty of Pharmaceutical Sciences, University of São Paulo (USP), 05508-000 São Paulo, Brazil

Hélder A. Santos
Department of Biomedical Engineering, University Medical Center Groningen, University of Groningen Ant. Deusinglaan 1, Groningen 9713 AV, The Netherlands; W.J. Kolff Institute for Biomedical Engineering and Materials Science, University Medical Center Groningen, University of Groningen Ant. Deusinglaan 1, Groningen 9713 AV, The Netherlands; Drug Research Program, Division of Pharmaceutical Chemistry and Technology, Faculty of Pharmacy, University of Helsinki, FI-00014 Helsinki, Finland

Marlus Chorilli
School of Pharmaceutical Sciences, São Paulo State University (UNESP), 14800-903 Araraquara, Brazil

Research Article

Keywords: High performance liquid chromatography; validation; thermogravimetry; lycopene; mesoporous silica nanoparticles

Posted Date: April 13th, 2023

DOI: https://doi.org/10.21203/rs.3.rs-2524778/v2

Abstract

Lycopene (LYC), a carotenoid extracted mainly from tomatoes, has several biological properties, making its use desirable as a nutraceutical and pharmaceutical active ingredient. However, the use of LYC in therapy has limitations related to its solubility and stability. In this study, mesoporous silica nanoparticles (MSNs) are used to load and protect LYC from degradation. The exact amount of drug incorporated was determined by analytical techniques, such as high performance liquid chromatography (HPLC) and thermal analysis. For this we developed and validated an HPLC method for LYC quantification and evaluated the LYC impregnated in MSNs, followed by thermogravimetry analysis (TGA) technique analysis. Differential scanning calorimetry (DSC) was also used in order to confirm drug incorporation. Additionally, an *in vitro* release study was also carried out. The HPLC method was duly validated for the range of 26–125 µg/mL and proved to be suitable for LYC quantification. DSC measurements suggest an improvement in the stability of the impregnated drug, which was reinforced by the release assay. Overall, the developed method is suitable to test LYC-loaded porous materials to enable the use in therapeutic applications.

1 Introduction

In view of lycopene (LYC) desirable biological properties, such as antimicrobial, antioxidant, antidiabetic, antihypercholesterolemic, anticancer, cardioprotective and photoprotector its use as nutraceutical and pharmaceutical active ingredient are increasingly being explored (Adetunji et al., 2021; Carvalho et al., 2021). However, this carotenoid, extracted mainly from tomato, has limitations related to its molecule, which is highly lipophilic, making it insoluble in aqueous solvents, hindering its use in therapy (Carvalho et al., 2020b; Khan et al., 2021). Therefore, alternatives have been studied, such as the use of nanotechnology. Despite the various options for nanocarriers, it is only possible to find studies associating LYC with organic nanocarriers, except for a study recently published by our group, where its association with inorganic nanocarriers is, until then, a field to be better explored (Carvalho et al., 2022, 2021, 2020b; Falsafi et al., 2021).

Among the various inorganics nanoparticles, mesoporous silica nanoparticles (MSNs) stand out as they present desirable properties, such as high thermal and chemical stabilities, large surface area, adjustable pore structure and particle diameter, free hydroxyls groups for functionalization, biocompatibility, biodegradability, low toxicity and easy elimination in living organisms, being widely applied in the biomedicine field (Carvalho et al., 2020c; Croissant et al., 2020; Fussell et al., 2014; Rahikkala et al., 2018). In order to develop a nanoformulation, several types of molecules can be incorporated, both in MSNs pores and on their surfaces by different ways, such as adsorption on the silica matrix, interaction with silanol groups and even through different functionalization possibilities (Croissant et al., 2017; Hoffmann et al., 2006; M Rosenholm et al., 2011).

It should be noted that the possibility of incorporation into the mesopores provides protection to the drug against environmental factors, which, in the context of providing the use of LYC in therapy, is extremely desirable since this drug can suffer degradation in contact with light, heat, oxygen and acidic environment (Kankala et al., 2019; Manzano and Vallet-Regí, 2020; Shi and Maguer, 2000). In order to guarantee the quality of the nanoformulation under development, knowing the amount of drug that the system is capable to load and its release profile (amount/time) is of fundamental importance, since these factors are directly linked to the drug content that will be available to interact with the target site (Carolina Alves et al., 2019; Carvalho et al., 2020b).

Although there are several analytical techniques for drug quantification, high performance liquid chromatography (HPLC) seems to be the most used (Carvalho et al., 2021, 2020b). HPCL is considered to be an easy separation and analysis method, which can be coupled to several types of detectors; however, the most explored is the ultraviolet detector (UV-Vis) (Hussain et al., 2019; Lucini et al., 2012; Montesano et al., 2008). In addition to HPLC, another essential technique also widely used for drug quantification is thermal analysis. This type of method has the ability to evaluate the structural and physical behaviour of samples through temperature (Cheremisinoff, 1996; Giron, 2002; Limnell et al., 2011). It is worth mentioning that in the literature it is possible to observe works where the quantification results obtained from HPLC showed good correlation with those obtained by thermal analysis, proving to be interesting the combination of these two techniques for the pharmaceutical development of new nanoformulations (Ceschel et al., 2003; Giron, 2002; Tsai et al., 2017). Thus, using these analytical techniques to determine the drug content in the incorporation and release tests, the present study seeks to develop a formulation based on mesoporous silica nanoparticles incorporated with LYC.

2 Methodology

2.1 Development and validation of an analytical method for LYC quantification

Firstly, tests with various mobile phase compositions, flow and injection volume were tested on a Waters e2695 HPLC instrument. The system consisted of a quaternary pump, a degasser, an autosampler, a column oven and a Waters 2998 model diode array detector (DAD). The best separation was achieved with a C18 column (250 mm × 4.6 mm, 5 µm), maintained at 35 ºC with mobile phase of acetonitrile:chloroform (89:11) (both with HPLC grade) at an isocratic flow of 2.0 mL/min, 20 µL injection volume and detection at 470 nm.

After defining the best method, the system suitability was evaluated according to the FDA "Validation of chromatographic methods" guide. Then, in order to determine the efficiency and suitability of the method with the intended use a validation was conducted in accordance with Q2 (R1) from International Conference on Harmonization, as described in **Table 1** (Carvalho et al., 2020a; FDA, 1994; International conference on harmonization, 2005).

2.2 Analytical method applicability: LYC-incorporated MSNs

Firstly, refluxed and calcined MSM (MSNs-R and MSNs-C, respectively) were synthesized according to a previous study and dried under vacuum for 1 h right before the impregnation process (Carvalho et al., 2022). Then, 5 mg of each were added in glass vials with LYC solutions (in chloroform) at different concentrations (1.0; 1.5; 2.0; 2.5; 3.0; 3.5; 4.0 mg/mL).

LYC solutions with MSNs were kept under stirring (100 RPM) for different times (6; 12; 24; 36; 48 h) under cooling (15^{o} C ± 5). After, LYC-loaded MSNs are centrifuged at 4000 rpm for 15 min and dried at room temperature under vacuum (Maturi et al., 2019; Sábio et al., 2019). The supernatant from the centrifugation was collected, filtered and analyzed by HPLC using the method under validation in order to determine the encapsulated efficacy percentage (EE%) and loading degree percentage (LD%), according to Equations 1 and 2 (Carolina Alves et al., 2019):

$$EE(\%) = \frac{\text{Total amount of drug added} - \text{Free amount in supernatant}}{\text{Total amount of drug added}} \times 100 \qquad (1)$$

$$LD(\%) = \frac{\text{Encapsulated drug}}{\text{Nanoparticle weight}} \times 100 \qquad (2)$$

In order to evaluate the incorporation methods statistical analyzes were performed, namely: stepwise regression of therms, t-test, ANOVA, Pareto graph, residual analysis, surface graph and contour analysis. All of them performed by the Minitab® software.

In parallel, the precipitate was analyzed by Thermogravimetric analysis (TGA). The TGA were obtained using a model TG-DSC 1 (Mettler Toledo). Purge gas of dry air atmosphere at a flow of 50 mL/min, heating rate of 10°C/min and temperature range of 30-800°C. The range Samples weighed about 3 mg and open alumina crucibles were used (Nascimento et al., 2019). Additionally, in order to characterize the nanoformulation it was also analyzed by differential scanning calorimetry (DSC), simultaneously with the TGA analysis, since the equipment used for this analysis was the same used for the TGA analysis.

Normalization of the samples was performed to provide a direct comparison of thermal curves. The LYC content on incorporated silica corresponds to a total mass variation (Δm_T) expressed as $\Delta m_T = \Delta m_S - \Delta m_{MSN}$, which is a product of subtracting the sample mass variation (ΔmS) by the empty silica (Δm_{MSN}), both measured after 170°C.

With the purpose of knowing the release profile of the system, a release study was carried out in a SteadyShake 757 Amerex® equipment, the samples (MSN@LYC and free LYC) remained throughout the test at a temperature of 37 ± 0.5 °C under constant agitation of 300 rpm (Rodero et al., 2018). In order to respect the sink condition, 1 mg of MSN@LYC and free LYC were added to 32.38 mL and 64.76 mL of acceptor medium, respectively (United States Pharmacopeia, 2020a). In order to mimic the vaginal environment, an acceptor medium composed of simulated vaginal fluid plus 2% of Span 60 and 5% of propanol was used, respecting the maximum quantity of organic solvent permitted by the US Pharmacopeia and the indication of using the lowest possible concentration of surfactant to reach the sink condition. It is worth noting that this acceptor medium had a pH of 4.5, compatible with the human vaginal pH (Marques et al., 2011; United States Pharmacopeia, 2020a). During the assay, 1 mL aliquots of samples were collected at predetermined times (0.25; 0.5; 1; 2; 4; 8; 12; 18; 24 and 32 h), in which 1 mL of acceptor medium was replaced. LYC content in the collected samples was quantified in a BioTek Epoch 2 microplate spectrophotometer at a fixed wavelength of 470 nm, which was previously partial validated.

3 Results And Discussion

3.1 Development and validation of an analytical method for LYC quantification

Initially, several methods already validated in the literature, with mobile phase composed of various combinations of water, acetonitrile and methanol were tested in a HPLC C18 column, which is shown to be the most used, together with C30, since, due to the fact that LYC is a nonpolar molecule interacts better with those types of columns (Carvalho et al., 2020b). However, it was not possible to reproduce those methods once the highest intensity peak (probably related to trans-LYC) was not well separated from the other LYC isomers (Amjad et al., 2020; Carvalho et al., 2020b; Mynul Hassan and Nam, 2021). As C18 columns have nonpolar stationary phase, ideally the mobile phase of choice would have to be composed of polar reagents, but in order to obtain a better spectrum (that best served the intended purpose), it was necessary to add an nonpolar solvent, like chloroform (Mynul Hassan and Nam, 2021; Vaudreuil et al., 2020).

As the developed method is meant to be used in the quantification of the total LYC incorporated in MSNs, it was opted for predominantly unite all isomers in a single peak, as shown in **Figure 1**. It is noteworthy that through the presence of the three characteristic peaks (approximately at 450, 470 and 505 nm) in the UV spectrum obtained, since the HPLC used is coupled to a DAD detector, it was possible to prove that such peak refers to LYC (Carvalho et al., 2020b).

After the method development, the system suitability was evaluated. This step is of fundamental importance since prior validation it is necessary to prove the method's performance quality and suitability for its intended use (FDA, 1994; United States Pharmacopeia, 2020b). According to USP 43, chapter 621, to assess the system suitability data from 5 injections of standard solutions must be compared, if the relative standard deviation (RSD) for the parameter under evaluation is ≤ 2.0%. Although, if the RSD is > 2.0, data from 6 injections should be evaluated. As can be seen in **Table 2**, data from 6 injections

were evaluated since more than one criterion showed RSD > 2.0 (United States Pharmacopeia, 2020b). It is noteworthy that the criteria were manually calculated according to formulas described in USP 43 and FDA.

Table 2: Assessment of the developed method system suitability for LYC quantification.

Chromatograms	Criteria				
	Retention time	Retention factor (K)	Theoretical plates	Symmetry factor	Tailing factor
1	7.14	3.80	10,160.64	1.57	1.37
2	7.17	4.02	7,024.12	1.60	1.33
3	7.05	3.90	9,391.26	1.80	1.17
4	7.17	3.92	9,178.88	1.60	1.32
5	7.10	3.80	4,676.79	1.33	1.13
6	7.07	3.85	6,777.00	1.43	1.33
Average	7.12	3.88	7,868.12	1.56	1.27
Standard deviation (SD)	0.05	0.08	1,887.73	0.15	0.09
RSD	0.69	1.98	23.99	9.49	7.21

In **Table 2** it can be seen that all mandatory criteria (retention factor, tailing factor and theoretical plates) are in accordance with the FDA recommendations (>2; ≤2; >2000, respectively), showing that the developed method is suitable and has excellent performance, being able to proceed to the validation step (FDA, 1994). Although the resolution criteria is mandatory, it is defined as the separation of two substances, as the purpose of this method is the quantification of a single substance, it could not be calculated. It is worth noting that although both, USP 43 and FDA, recommend the calculation of the asymmetry factor as it is not a mandatory item, they do not provide an acceptable limit for it (FDA, 1994; United States Pharmacopeia, 2020b).

3.2 Analytical methodology validation

3.2.1 Linearity

In the linear regression analysis (**Figure 2**), it was possible to observe that there was a good correlation between the two variables, as the R^2 was greater than 0.990 and the slope was significantly different from zero, suggesting that the results have linearity. Additionally, analysis of variance (ANOVA) was performed for the statistical evaluation of the residuals, using a significance level of 5%, been possible to confirm their homoscedasticity, as they are randomly distributed (**Figure 3**).

Table 3 shows that the data are accordingly with the recommended range to be accurate, as the percentage of recovery is within the range of 100 ± 20%, so it can be considered that the method is accurate for the evaluated range (25.0–125.0 µg/mL) (International conference on harmonization, 2005).

Table 3: Results obtained from the method validation and its respective recovery percentage.

Concentration (ug/mL)	Replicas (area value)			Average	SD	RSD	Experimental concentration	Accuracy (%)
	1	2	3					
125	4685072	4634211	4505611	4608298.00	92494.190	2.00	118.755	95.004
75	2448638	2537891	2484637	2490388.667	44903.630	1.803	67.641	90.188
25	696659	725397	681434	701163.333	22324.943	3.183	24.460	97.840

3.2.3 Precision

As it can be seen in **Table 4**, all the concentrations evaluated met the precision criterion, since all RSD were below 5 (International conference on harmonization, 2005; Perez, 2010).

Table 4: Precision data performed on different days by a single analyst.

Concentration (µg/mL)	Replicas			Average	SD	RSD
	Day 1	Day 2	Day 3			
125	4847745	4687509	4816669	4783974	84974.11	1.78
75	2739102	2642411	2587778	2656430	76629.92	2.88
25	723325	705900	702876	710700,3	11037.34	1.55

Additionally, in the intermediate precision analysis, the method was reproducible through the proximity of the standard deviation of the two analysts (below 5) (**Table 5**) and by both coefficient of variation being above 0.990 (**Figure 4**) (International conference on harmonization, 2005).

Table 5: Average comparison of the precision data obtained by two analysts.

	Analyst 1					Analyst 2					Comparison between analysts	
Concentration (µg/mL)	Day 1	Day 2	Day 3	Average	RSD	Day 1	Day 2	Day 3	Average	RSD	Average	RSD
125	4847745	4687509	4816669	4783974.0	1.78	4628742	4392490	4421263	4480831.667	2.88	4632403.000	4.627
75	2739102	2642411	2587778	2656430.0	2.88	2765615	2688520	2522324	2658819.667	4.68	2657625.000	0.063
25	723325	705900	702876	710700.3	1.55	770031	709346	759136	746171.000	4.34	728435.666	3.443

3.2.4 Detection limit (DL) and quantification limit (QL)

The values obtained for DL and QL were 8.58 and 26.00 µg/mL, respectively, since the value obtained for the residual standard deviation of the linear regression was 107755.2877 and the value obtained for the slope of the linear regression line was 41435. On the one hand, it can be stated that the method under validation allows the detection of samples with a LYC content of at least 8.58 µg/mL, and its quantification from 26 µg/mL. On the other hand, the lowest concentration evaluated during the validation process, 25 µg/mL, was determined with accuracy and precision, but when lower concentrations were tested, precise results were not detected (FDA, 1994; International conference on harmonization, 2005). It is worth noting that experimental determinations are less reliable than calculated ones, since there is the operator variability in several steps, such as weighing and pipetting (Carvalho et al., 2020a; Vial and Jardy, 1999). In order to minimize operational errors in QL and DL experimental determination correction values were used. Those values are based on experimental standard deviation values of an number of ideal replicas, *e.g.*, the values of 3.3 and 10 in QL and DL formulas mentioned previously, respectively (Vial and Jardy, 1999). Thus, it is possible to consider, with a higher level of reliability, by disregarding the operational error, that the QL for the method under validation is 26 µg/mL.

3.2.5 Range

Based on the results presented for the linearity, precision and accuracy criteria and taking into account the QL result the range of the method under validation is 26-125 µg/mL (International conference on harmonization, 2005).

3.2.6 Robustness

The data in **Table 6** shows the area obtained after small and deliberate variations of certain parameters, as well as its evaluation according to the accuracy criterion. In all tested variations, the recovery percentage complied with the acceptance criterion of 100 ± 20%, proving the method robustness (International conference on harmonization, 2005).

Table 6: Robustness results, at medium concentration, for the developed method.

Parameters	Variations	Replica			Average	RSD	Experimental concentration (µg/mL)	Accuracy (%)
		1	2	3				
Injection	22 µL	2879636	2852237	3052237	2928036.667	3.70	78.20	104.3
	18 µL	2411787	2412978	2375422	2400062.333	0.89	65.46	87.3
Column oven temperature	33 ºC	2551764	2550736	2568953	2557151.000	0.40	69.25	92.3
	37 ºC	2581679	2531772	2552768	2555406.333	0.98	69.21	92.3
Flow	1.8 mL/min	2535050	2537438	2567236	2546574.667	0.70	69.00	92.0
	2.2 mL/min	2523317	2511055	2501068	2511813.333	0.44	68.16	90.9
Mobile phase composition	Acetonitrile:chloroform 87:13	2657224	2721932	2749512	2709556.000	1.75	72.93	97.2
	Acetonitrile:chloroform 91:9	2562622	2584182	2574104	2573636.000	0.42	69.65	92.9

3.2.7 Selectivity (specificity)

The method proved to be selective in quantifying LYC in the presence of both MSN-C and MSN-R, since only the baseline was observed. Additionally, the solvent (chloroform) non-interference was also proven for the same reason. In the degradation study, in order to verify the degradation products interference, exposure to oxygen and temperature did not significantly change the analyte recovery, since both were within the allowed, 100 ± 20% (Table 7). In **Figure 5**, after temperature degradation, there was a peak broadening, which can be explained by the cis-trans isomerization caused by this type of degradation, since during the development of the method it was chosen to unite the isomers. This justifies the non-appearance of additional peaks (Carvalho et al., 2020b; Shi and Maguer, 2000).

Degradation studies	Average area	Experimental concentration (µg/mL)	Recovery (%)
Oxygen	2388977.000	65.19	86.9
Temperature	2729366.667	73.41	97.9
Visible light	966014.666	30.85	41.1
UV light	175233.000	11.77	15.7
pH 7.6	2062346.000	57.31	76.4
pH 8.5	4240115.000	109.87	146.5

Table 7: Degradation studies results carried out to assess the specificity of the developed method.

In the visible and UV light degradation spectra it was observed not only a lower analyte recovery percentage but also a lower peak intensity, which is in agreement with the literature data as light degradation causes a reduction in the total LYC content (both cis and trans) by oxidation. Moreover, in the case of temperature degradation, this reduction is caused by isomerization, which produce other degradation products that are probably not detected in the wavelength used (SHI et al., 2003; Tahmasebi and Emam-Djomeh, 2021). Finally, the change in the sample pH can be considered the limitation of this study, since, because chloroform is volatile, the measurement of the solution by a pH-meter was compromised by the non-stabilization of the value. In addition, the reading by a pH strip was also compromised as the sample has color, making the reading difficult. It is worth mentioning that the standard LYC solution (solubilized in the mobile phase) had a pH around 6 and is therefore considered acidic. Once LYC is degraded in acidic medium, the greater intensity observed in the sample peak at pH 8.5 is coherent, and, consequently, the greater recovery obtained (**Table 7** and **Figure 5**). Finally, it is worth mentioning that the LYC chemical reference substance and LYC for analysis (used in the application part) spectra did not display any significant difference.

3.3 Analytical method applicability: LYC-incorporated MSNs

Table 8 shows the average results obtained for all LYC-incorporated MSNs conditions. It is worth noting that the concentrations above the validated range were diluted and the analysis were repeated. As there are no previous studies in the literature regarding the incorporation of LYC in this type of nanoparticle making a parallel is complicated because the amount of drug that is incorporated depends on the interaction between LYC and MSNs carrier, in addition to characteristics inherent to the silica matrix such as surface area and pore size and structure (Carvalho et al., 2020b; Croissant et al., 2017; Deodhar et al., 2017; Falsafi et al., 2021; Hoffmann et al., 2006; M Rosenholm et al., 2011). However, it can be observed that both MSNs had similar values of EE% and LD% under the same conditions, and that in some conditions the EE% value was close to 100%, which confirms that LYC was successfully incorporated into both MSNs.

MSN type/ Concentration (mg/mL)	Time														
	6h			12h			24 h			36 h			48h		
	Free LYC (mg/mL)	EE%	LD%	Free LYC (mg/mL)	EE%	LD%	Free LYC (mg/mL)	EE%	LD%	Free LYC (mg/mL)	EE%	LD%	Free LYC (mg/mL)	EE%	LD%
MSN-R/1.0	0.377	62.2	12.4	0.533	46.6	9.3	0.658	34.1	6.8	0.504	49.5	9.9	0.145	85.4	17.0
MSN-R/1.5	0.920	38.6	11.5	0.505	66.3	19.8	0.839	44.0	13.2	0.849	43.3	13.0	0.041	97.2	29.1
MSN-R/2.0	0.897	55.1	22.0	0.754	62.2	24.9	0.548	72.5	29.0	0.530	73.3	29.3	0.024	98.7	39.5
MSN-R/2.5	1.405	43.7	21.8	0.696	72.1	36.0	0.833	66.6	33.3	0.660	73.5	36.7	0.045	98.1	49.0
MSN-R/3.0	1.185	60.4	36.2	0.784	73.8	44.3	0.322	89.2	53.5	0.115	96.1	57.6	0.008	99.7	59.8
MSN-R/3.5	1.412	59.6	41.7	0.999	71.4	50.0	0.236	93.2	65.2	0.065	98.1	68.6	0.063	98.1	68.7
MSN-R/4.0	1.484	62.8	50.3	0.810	79.7	63.7	0.365	90.8	72.6	0.067	98.3	78.6	0.003	99.9	79.9
MSN-C/1.0	0.463	53.6	10.7	0.578	42.1	8.4	0.245	75.4	15.0	0.550	44.9	8.9	0.494	50.6	10.1
MSN-C/1.5	0.703	53.0	15.9	0.608	59.4	17.8	0.293	80.4	24.1	0.847	43.5	13.0	0.239	84.0	25.2
MSN-C/2.0	1.091	45.4	18.1	0.616	69.1	27.4	0.984	50.7	20.3	1.149	42.5	17.0	0.079	96.0	38.4
MSN-C/2.5	1.223	51.0	25.5	0.837	66.5	33.2	0.904	63.8	31.9	1.409	43.6	21.8	0.616	75.3	37.6
MSN-C/3.0	1.226	59.1	35.4	1.257	64.0	34.8	0.627	79.0	47.4	0.379	87.0	52.4	0.323	89.2	53.5
MSN-C/3.5	1.313	62.4	43.7	1.033	70.4	49.3	0.694	80.1	56.1	0.212	94.1	65.7	0.706	79.8	55.8
MSN-C/4.0	1.942	51.4	41.1	1.399	65.0	52.0	0.376	90.5	72.4	0.177	93.7	76.4	0.747	81.3	65.0

Table 8: Average results obtained for all LYC-incorporated MSNs conditions evaluated.

During the statistical analysis, the p-value obtained was much lower than the Student's *t*-value (for both MSNs studied), been that the time and concentration variables interfere differently for the EE%. These results can be confirmed by the Pareto chart and by the surface graph (**Figure 6 A and B**). Additionally, the residuals ANOVA test confirmed that these data are homoscedastic, which increases the data reliability **(Figure 6 E and F)**.

In addition, the statistical analysis of the LD% data for the MSNs-R showed that the variables concentration and concentration with time interfere significantly for the LD% results. However, the isolated time variable does not significantly interfere because in addition to the Student's *t*-value be higher than the p-value (-0.20 and 0.839, respectively) the Pareto graph and the surface graph also reinforce this information (**Figure 7 A, C, E**). Additionally, the ANOVA test residuals confirmed that these data are homoscedastic, which increases the reliability of these findings.

In MSN-C LD% results, both variables showed to interfere significantly to the LD%, but this same pattern was not observed in their associations. Pareto graph and the surface graph also reinforce this information (**Figure 7 B, D, F**). Additionally, the residuals ANOVA test confirmed that these data are homoscedastic, which increases their reliability. This difference in LD% between the two types of MSNs studied is not very clear in the literature, but a possible reason for a lower LD% value to MSN-C may be because during calcination there is repulsion between the silanol groups on its surface, which can cause aggregation, decreasing not only its dispersion in the solvent used for the incorporation step, but also the surface area available for drug loading (Ghasemi et al., 2017; Lin et al., 2012; Wu et al., 2013).

3.4 TGA analysis

Figure 8A shows the thermal behavior of LYC, MSN-C, and MSN-R up to 800ºC. LYC thermal decomposition was observed starting at 170°C, which presented 100% of mass loss in the TGA curve. Both silica showed mass losses before LYC onset temperature of thermal decomposition, steps attributed to dehydration of the samples and discarded from calculations. Above this temperature, different total mass losses were also observed for calcinated (3.33%) and refluxed (4.67%) MSN, these values were attributed to the decomposition of organic matter.

The standard in the concentration increase can be observed with the increase of the total mass loss in the TGA curve (**Figure 8B**) and in the thermal data summarized in **Table 9**. The behavior of MSN-R at 48h is representative of all samples studied in this work. The thermal profile of the samples is similar since the matrix is the same for all of them. Nevertheless, the sample at concentration 4.0 mg/mL presented a lower mass loss until 170ºC, with made the curve overlap with its predecessor at concentration 3.5 mg/mL. Anyway, the total mass loss between 170-800 ºC still been higher for concentration 4.0 mg/mL. Additionally, **Figure 8C** shows the incorporated sample before and after the thermal analysis. As can be observed it has a color change after 800ºC, which suggests that all organic matter correlated to LYC has been burned.

Table 9: Thermal data of incorporated silica in different times.

MSN type/ Concentration (mg/mL)	6h		12h		24h		36h		48h	
	Mass loss (%)	Δm_T %	Mass loss (%)	Δm_T %	Mass loss (%)	Δm_T %	Mass loss (%)	Δm_T %	Mass loss (%)	Δm_T %
MSN-R/1.0	5.94	1.27	12.13	7.46	9.38	4.71	10.83	6.16	11.75	7.08
MSN-R/1.5	10.53	5.86	12.73	8.06	11.41	6.74	12.15	7.48	13.84	9.17
MSN-R/2.0	14.24	9.57	13.60	8.93	13.21	8.54	16.11	11.44	15.74	11.07
MSN-R/2.5	17.06	12.39	12.80	8.13	13.52	8.85	16.87	12.20	15.62	10.95
MSN-R/3.0	17.22	12.55	14.48	9.81	15.68	11.01	17.98	13.31	16.49	11.82
MSN-R/3.5	17.92	13.25	15.78	11.11	16.33	11.66	18.68	14.01	20.23	15.56
MSN-R/4.0	19.59	14.92	18.54	13.87	19.47	14.80	19.85	15.18	20.59	15.92
MSN-C/1.0	5.70	2.37	7.49	4.16	5.58	2.25	5.78	2.45	5.02	1.69
MSN-C/1.5	6.83	3.50	9.64	6.31	9.02	5.69	7.18	3.85	8.85	5.52
MSN-C/2.0	7.50	4.17	11.31	7.98	9.17	5.84	8.64	5.31	12.04	8.71
MSN-C/2.5	7.73	4.40	12.03	8.70	12.15	8.82	11.77	8.44	12.82	9.49
MSN-C/3.0	10.37	7.04	13.82	10.49	14.59	11.26	13.88	10.55	14.88	11.55
MSN-C/3.5	10.47	7.14	14.27	10.94	14.91	11.58	14.14	10.81	15.25	11.92
MSN-C/4.0	13.73	10.4	14.70	11.37	15.24	11.91	16.57	13.24	16.48	13.15

Although the thermal analysis was able to quantify the amount of drug in the systems, as the LYC content (represented by Δm_T) and for also follows the same linearity pattern observed for the HPLC, the higher the concentration of the incorporation solution, the greater the amount of incorporated drug, it is possible to observe in **Figures 9** and **10** that the value was significantly lower than the LD% obtained by HPLC. Despite there are studies in the literature addressing the good results correlation between TGA and HPLC quantification, this fact was not observed in this study (Almaghrabi et al., n.d.; Christoforidou et al., 2021; Tamasi et al., 2021; Zhang et al., 2010). A possible justification for this fact is that the technique used to determine the EE% and LD% by HPLC was the indirect technique, while the thermal analysis was the direct one. It is possible to observe in the literature studies whose objective was to compare different drug incorporation methods, which observed that in the indirect method the quantification was greater than the one observed by the direct method, which is in agreement with the results obtained here (Amini et al., 2017; Bakonyi et al., 2017; Keawchaoon and Yoksan, 2011). Being the indirect method considered more reliable by some authors, mainly due to the smallest standard deviation and reproducibility (between different indirect methods) (Amini et al., 2017; Bakonyi et al., 2017; Khoshneviszadeh et al., 2016). However, those information does not seem to be a consensus in the literature (Daneshmand et al., 2018; de Câmara et al., 2016).

3.5 *Contour analysis*

Additionally, contour analysis (**Figure 11**) was performed to assist in the decision making as it illustrates the relationship between time and concentration. Emphasis was placed on the ideal incorporation of 2.5 mg/mL (this ideal incorporation value was defined based on previous studies according to a specific application, the anti-candida one) (Carvalho et al., 2022). Taking into account the conditions tested and the inherent cost of the drug, it can be said that the ideal incorporation condition for the MSN-R is 2.5 mg/mL and 3.0 mg/mL for 48 h for MSN-C. However, due to the fact that the MSN-R presents better DL% results and allows the ideal incorporation with a smaller amount of drug, the MSN@LYC (incorporated with 2.5 mg/mL of drug for 48h) was chosen for the following experiments, being called only MSN@LYC.

3.6 *Differential scattering calorimetry (DSC)*

In addition to the TGA, in the incorporation condition considered as ideal, the DSC curve was performed (**Figure 12**), as well for the MSN-R and the free drug. It is possible to observe that the three DSC curves have a first endothermic event (up to 150 °C), attributed to loss of water or solvents adsorbed in the samples (Maturi et al., 2019). According to the literature, lycopene may have two possible melting points, the first in the region of 169.48 °C, referring to the cis isomer, and the second around 176.35 °C, referring to the trans isomer. According to LYC manufacturer (APIChem Technology Co.), the active pharmaceutical ingredient used here is composed only of the trans isomer (purity of 98.2% according to the report provided by the manufacturer), which therefore agrees with the endothermic peak observed around 180-190 °C in the DSC curves for free LYC and MSN@LYC (with almost imperceptible intensity in the latter) (Murakami et al., 2017; Takehara et al., 2014). This almost imperceptible intensity may suggest a change in the crystalline network, indicating that it is in the amorphous state within the mesopores of the MSN (Akhoond Zardini et al., 2018; Pu and Tang, 2017).

In the DSC curve of free LYC, it is also possible to observe an exothermic event around 240°C, which, according to the literature, refers to the thermal decomposition of the drug (Pu and Tang, 2017). This event was not observed in the MSN@LYC curve, indicating the occurrence of interaction between the drug and the nanoparticle. It is also worth noting that this fact also indicates that the incorporation provided greater stability to the drug, which, after incorporation, began to be degraded at approximately 350 °C. This profile mentioned here is an indication that LYC is inside the MSN mesopores (Pu and Tang, 2017).

3.7 *In vitro* release assay

As can be seen in **Figure 13**, while the system was able to release 97.79% of the drug in 12 h and 100% in 24 h of the experiment, the free drug released 39.03% in 32 h. A comparison with the literature is difficult since studies involving MSN with LYC are rare and the release profile is closely linked with the interactions between drug and nanoparticle. However, it is possible to suggest that the profile observed here differs slightly from those presented in the literature for this type of nanoparticle, such as in the work of Bolouki et al., (2015), who studied the release profile of MSN incorporated with curcumin, in different pH, through a methodology similar to the one used here, and observed that none of them reached a release of 100% (the maximum observed was 40-45%); however, around 8 to 10 h, a value close to the final release was reached.

However, in a similar study approaching the release profile of ibuprofen incorporated in different MSNs (the authors synthesized four types of MSNs varying the microwave power in the range of 100-450 W) it was observed that all of them needed 50 h to reach a 100% of drug release. Around 20 h, all formulations showed a release of 70-90% of the drug (Kamarudin et al., 2014). Similarly, Peretti et al., (2018) evaluated the release profile of MSN incorporated with pentamidine and observed a release of 90% in 25 h. It is also worth mentioning that a rapid release (around 80% of the total drug) occurred in the first hours of the experiment (a little before 6 h).

Finally, it is worth mentioning that the use of the microplate reader was preferable for this assay, since the detection limit (determined experimentally during partial validation) was 4.6 µg/mL, well below that obtained with the HPLC method.

4 Conclusion

When it comes to the development of a new nanoformulation, the use of analytical techniques in order both to characterize the system and to predict its behavior in a future human application is of fundamental importance. The HPLC method developed here proved to be linear, accurate, precise and robust, in addition to being selective under the tested conditions, including its application for LYC quantification. So, it can be said that the developed method was duly validated for the range of 26–125 µg/mL. However, it proved to be suitable for applicability in the quantification of content for incorporation conditions tested. A parallel with the TGA analysis was perhaps the limitation of this study. Additionally, by DSC it is possible to suggest that the incorporation of the drug in the mesopores was carried out, and that it protects the drug from degradation. This result is in agreement with the results of the release test, where the protection of the drug by the nanoparticle was also evident. These findings make MSN a promising nanocarrier for LYC incorporation in order to circumvent the limitations of using this drug in therapy, since it has several pharmacological actions described in the literature.

Declarations

5 ACKNOWLEDGEMENTS

This work was supported by São Paulo Research Foundation (FAPESP, Brazil) grant numbers nº 2019/26821-7; 2018/23357-5, 2019/09831-9 and 2018/25377-3, and the UMCG Research Funds.

References

Adetunji, C.O., Akram, M., Mtewa, A.G., Jeevanandam, J., Egbuna, C., Ogodo, A.C., Gautam, A.K., Gupta, A., Onyekere, P.F., Tupas, G.D., others, 2021. Biochemical and pharmacotherapeutic potentials of lycopene in drug discovery, in: Preparation of Phytopharmaceuticals for the Management of Disorders. Elsevier, pp. 307–360.

Akhoond Zardini, A., Mohebbi, M., Farhoosh, R., Bolurian, S., 2018. Production and characterization of nanostructured lipid carriers and solid lipid nanoparticles containing lycopene for food fortification. J. Food Sci. Technol. 55, 287–298. https://doi.org/10.1007/s13197-017-2937-5

Almaghrabi, M., Alqurshi, A., Jadhav, S.A., Mazzacuva, F., Cilibrizzi, A., Raimi-Abraham, B., Royall, P.G., n.d. Evaluating Thermogravimetric Analysis for the Measurement of Drug Loading in Mesoporous Silica Nanoparticles (MSNs). Available SSRN 4355731.

Amini, Y., Amel Jamehdar, S., Sadri, K., Zare, S., Musavi, D., Tafaghodi, M., 2017. Different methods to determine the encapsulation efficiency of protein in PLGA nanoparticles. Biomed. Mater. Eng. 28, 613–620. https://doi.org/10.3233/BME-171705

Amjad, M., Hussain, S., Rehman Khan, A., 2020. Development and Validation of HPLC assay of Lycopene in Different Matrices. World J. Appl. Chem. 5, 26. https://doi.org/10.11648/j.wjac.20200502.13

Bakonyi, M., Berkó, S., Budai-Szűcs, M., Kovács, A., Csányi, E., 2017. DSC for evaluating the encapsulation efficiency of lidocaine-loaded liposomes compared to the ultracentrifugation method. J. Therm. Anal. Calorim. 130, 1619–1625. https://doi.org/10.1007/s10973-017-6394-1

Bolouki, A., Rashidi, L., Vasheghani-Farahani, E., Piravi-Vanak, Z., 2015. Study of mesoporous silica nanoparticles as nanocarriers for sustained release of curcumin. Int. J. Nanosci. Nanotechnol. 11, 139–146.

Carolina Alves, R., Perosa Fernandes, R., Fonseca-Santos, B., Damiani Victorelli, F., Chorilli, M., 2019. A Critical Review of the Properties and Analytical Methods for the Determination of Curcumin in Biological and Pharmaceutical Matrices. Crit. Rev. Anal. Chem. 49, 138–149. https://doi.org/10.1080/10408347.2018.1489216

Carvalho, G.C., Bugno, A., Almodovar, A.A.B., Silva, F.P. de L. e, Pinto, T. de J.A., 2020a. Validation and applicability of an alternative method for dialysis water and dialysate quality analysis. Brazilian J. Nephrol. 42, 163–174. https://doi.org/10.1590/2175-8239-jbn-2019-0203

Carvalho, G.C., de Camargo, B.A.F., de Araújo, J.T.C., Chorilli, M., 2021. Lycopene: From tomato to its nutraceutical use and its association with nanotechnology. Trends Food Sci. Technol. 118, 447–458. https://doi.org/10.1016/j.tifs.2021.10.015

Carvalho, G.C., Marena, G.D., Leonardi, G.R., Sábio, R.M., Corrêa, I., Chorilli, M., Bauab, T.M., 2022. Lycopene, Mesoporous Silica Nanoparticles and Their Association: A Possible Alternative against Vulvovaginal Candidiasis? Molecules 27, 8558. https://doi.org/10.3390/molecules27238558

Carvalho, G.C., Sábio, R.M., Chorilli, M., 2020b. An Overview of Properties and Analytical Methods for Lycopene in Organic Nanocarriers. Crit. Rev. Anal. Chem. 1–13. https://doi.org/10.1080/10408347.2020.1763774

Carvalho, G.C., Sábio, R.M., de Cássia Ribeiro, T., Monteiro, A.S., Pereira, D.V., Ribeiro, S.J.L., Chorilli, M., 2020c. Highlights in Mesoporous Silica Nanoparticles as a Multifunctional Controlled Drug Delivery Nanoplatform for Infectious Diseases Treatment. Pharm. Res. 37, 191. https://doi.org/10.1007/s11095-020-02917-6

Ceschel, G.., Badiello, R., Ronchi, C., Maffei, P., 2003. Degradation of components in drug formulations: a comparison between HPLC and DSC methods. J. Pharm. Biomed. Anal. 32, 1067–1072. https://doi.org/10.1016/S0731-7085(03)00210-3

Cheremisinoff, N.P., 1996. Polymer Characterization Laboratory Techniques and Analysis. Westwood, New Jersey. https://doi.org/10.1016/B978-0-8155-1403-9.50004-2

Christoforidou, T., Giasafaki, D., Andriotis, E.G., Bouropoulos, N., Theodoroula, N.F., Vizirianakis, I.S., Steriotis, T., Charalambopoulou, G., Fatouros, D.G., 2021. Oral Drug Delivery Systems Based on Ordered Mesoporous Silica Nanoparticles for Modulating the Release of Aprepitant. Int. J. Mol. Sci. 22, 1896. https://doi.org/10.3390/ijms22041896

Croissant, J.G., Butler, K.S., Zink, J.I., Brinker, C.J., 2020. Synthetic amorphous silica nanoparticles: toxicity, biomedical and environmental implications. Nat. Rev. Mater. 5, 886–909. https://doi.org/10.1038/s41578-020-0230-0

Croissant, J.G., Fatieiev, Y., Khashab, N.M., 2017. Degradability and clearance of silicon, organosilica, silsesquioxane, silica mixed oxide, and mesoporous silica nanoparticles. Adv. Mater. 29, 1604634.

Daneshmand, S., Golmohammadzadeh, S., Jaafari, M.R., Movaffagh, J., Rezaee, M., Sahebkar, A., Malaekeh-Nikouei, B., 2018. Encapsulation challenges, the substantial issue in solid lipid nanoparticles characterization. J. Cell. Biochem. 119, 4251–4264. https://doi.org/10.1002/jcb.26617

de Câmara, A.A., Dupont, S., Beney, L., Gervais, P., Rosenthal, A., Correia, R.T.P., Pedrini, M.R. da S., 2016. Fisetin yeast-based bio-capsules via osmoporation: effects of process variables on the encapsulation efficiency and internalized fisetin content. Appl. Microbiol. Biotechnol. 100, 5547–5558. https://doi.org/10.1007/s00253-016-7425-8

Deodhar, G. V, Adams, M.L., Trewyn, B.G., 2017. Controlled release and intracellular protein delivery from mesoporous silica nanoparticles. Biotechnol. J. 12, 1600408.

Falsafi, S.R., Rostamabadi, H., Babazadeh, A., Tarhan, Ö., Rashidinejad, A., Boostani, S., Khoshnoudi-Nia, S., Akbari-Alavijeh, S., Shaddel, R., Jafari, S.M., 2021. Lycopene nanodelivery systems; recent advances. Trends Food Sci. Technol.

FDA, R.G., 1994. Validation of chromatographic methods. Cent. Drug Eval. Res. (CDER), Washington, USA.

Fussell, A.L., Mah, P.T., Offerhaus, H., Niemi, S.-M., Salonen, J., Santos, H.A., Strachan, C., 2014. Coherent anti-Stokes Raman scattering microscopy driving the future of loaded mesoporous silica imaging. Acta Biomater. 10, 4870–4877. https://doi.org/10.1016/j.actbio.2014.07.021

Ghasemi, S., Farsangi, Z.J., Beitollahi, A., Mirkazemi, M., Rezayat, S.M., Sarkar, S., 2017. Synthesis of hollow mesoporous silica (HMS) nanoparticles as a candidate for sulfasalazine drug loading. Ceram. Int. 43, 11225–11232. https://doi.org/10.1016/j.ceramint.2017.05.172

Giron, D., 2002. Applications of thermal analysis and coupled techniques in pharmaceutical industry. J. Therm. Anal. Calorim. 68, 335–357.

Hoffmann, F., Cornelius, M., Morell, J., Fröba, M., 2006. Cover Picture: Silica-Based Mesoporous Organic–Inorganic Hybrid Materials (Angew. Chem. Int. Ed. 20/2006). Angew. Chemie Int. Ed. 45, 3187.

Hussain, A., Pu, H., Sun, D.W., 2019. Measurements of lycopene contents in fruit: A review of recent developments in conventional and novel techniques. Crit. Rev. Food Sci. Nutr. 59, 758–769. https://doi.org/10.1080/10408398.2018.1518896

International conference on harmonization, 2005. Validation of analytical procedures: text and methodology Q2 (R1), in: International Conference on Harmonization, Geneva, Switzerland.

Kamarudin, N.H.N., Jalil, A.A., Triwahyono, S., Artika, V., Salleh, N.F.M., Karim, A.H., Jaafar, N.F., Sazegar, M.R., Mukti, R.R., Hameed, B.H., Johari, A., 2014. Variation of the crystal growth of mesoporous silica nanoparticles and the evaluation to ibuprofen loading and release. J. Colloid Interface Sci. 421, 6–13.

https://doi.org/10.1016/j.jcis.2014.01.034

Kankala, R.K., Zhang, H., Liu, C.-G., Kanubaddi, K.R., Lee, C.-H., Wang, S.-B., Cui, W., Santos, H.A., Lin, K., Chen, A.-Z., 2019. Metal species–encapsulated mesoporous silica nanoparticles: current advancements and latest breakthroughs. Adv. Funct. Mater. 29, 1902652.

Keawchaoon, L., Yoksan, R., 2011. Preparation, characterization and in vitro release study of carvacrol-loaded chitosan nanoparticles. Colloids Surfaces B Biointerfaces 84, 163–171. https://doi.org/10.1016/j.colsurfb.2010.12.031

Khan, U.M., Sevindik, M., Zarrabi, A., Nami, M., Ozdemir, B., Kaplan, D.N., Selamoglu, Z., Hasan, M., Kumar, M., Alshehri, M.M., Sharifi-rad, J., 2021. Review Article Lycopene : Food Sources , Biological Activities , and Human Health Benefits 2021.

Khoshneviszadeh, R., FAZLY, B.B.S., Housaindokht, M.R., EBRAHIM, H.A., Rajabi, O., 2016. A comparison of explanation methods of encapsulation efficacy of hydroquinone in a liposomal system.

Limnell, T., Heikkilä, T., Santos, H.A., Sistonen, S., Hellstén, S., Laaksonen, T., Peltonen, L., Kumar, N., Murzin, D.Y., Louhi-Kultanen, M., Salonen, J., Hirvonen, J., Lehto, V.-P., 2011. Physicochemical stability of high indomethacin payload ordered mesoporous silica MCM-41 and SBA-15 microparticles. Int. J. Pharm. https://doi.org/10.1016/j.ijpharm.2011.06.050

Lin, Y.-S., Hurley, K.R., Haynes, C.L., 2012. Critical Considerations in the Biomedical Use of Mesoporous Silica Nanoparticles. J. Phys. Chem. Lett. 3, 364–374. https://doi.org/10.1021/jz2013837

Lucini, L., Pellizzoni, M., Baffi, C., Molinari, G. Pietro, 2012. Rapid determination of lycopene and β-carotene in tomato by liquid chromatography/electrospray tandem mass spectrometry. J. Sci. Food Agric. 92, 1297–1303. https://doi.org/10.1002/jsfa.4698

M Rosenholm, J., Sahlgren, C., Lindén, M., 2011. Multifunctional mesoporous silica nanoparticles for combined therapeutic, diagnostic and targeted action in cancer treatment. Curr. Drug Targets 12, 1166–1186.

Manzano, M., Vallet-Regí, M., 2020. Mesoporous silica nanoparticles for drug delivery. Adv. Funct. Mater. 30, 1902634.

Marques, M.R.C., Loebenberg, R., Almukainzi, M., others, 2011. Simulated biological fluids with possible application in dissolution testing. Dissolution Technol 18, 15–28.

Maturi, F.E., Sábio, R.M., Silva, R.R., Lahoud, M.G., Meneguin, A.B., Valente, G.T., Caface, R.A., Leite, I.S., Inada, N.M., Ribeiro, S.J.L., 2019. Luminescent Mesoporous Silica Nanohybrid Based on Drug Derivative Terbium Complex. Materials (Basel). 12, 933.

Mayeaux, M., Xu, Z., King, J.M., Prinyawiwatkul, W., 2006. Effects of Cooking Conditions on the Lycopene Content in Tomatoes. J. Food Sci. 71, C461–C464. https://doi.org/10.1111/j.1750-3841.2006.00163.x

Montesano, D., Fallarino, F., Cossignani, L., Bosi, A., Simonetti, M.S., Puccetti, P., Damiani, P., 2008. Innovative extraction procedure for obtaining high pure lycopene from tomato. Eur. Food Res. Technol. 226, 327–335. https://doi.org/10.1007/s00217-006-0541-4

Murakami, K., Honda, M., Takemura, R., Fukaya, T., Kubota, M., Wahyudiono, Kanda, H., Goto, M., 2017. The thermal Z-isomerization-induced change in solubility and physical properties of (all-E)-lycopene. Biochem. Biophys. Res. Commun. 491, 317–322. https://doi.org/10.1016/j.bbrc.2017.07.103

Mynul Hassan, M., Nam, S.-W., 2021. High-Performance Liquid Chromatography for Determining a Mixture of Nonsteroidal Anti-inflammatory Drugs. Electron. Mater. Lett. 17, 414–420. https://doi.org/10.1007/s13391-021-00306-8

Nascimento, A.L.C.S., Ashton, G.P., Parkes, G.M.B., Ekawa, B., Fernandes, R.P., Carvalho, A.C.S., Ionashiro, M., Caires, F.J., 2019. Novel solid-state compounds of heavy rare-earth (III) picolinates. A pyrolytic study using: TG-DSC-IR, HSM-MS and GC-MS. J. Anal. Appl. Pyrolysis 144, 104709. https://doi.org/10.1016/j.jaap.2019.104709

Peretti, E., Miletto, I., Stella, B., Rocco, F., Berlier, G., Arpicco, S., 2018. Strategies to Obtain Encapsulation and Controlled Release of Pentamidine in Mesoporous Silica Nanoparticles. Pharmaceutics 10, 195. https://doi.org/10.3390/pharmaceutics10040195

Perez, M.Â.F., 2010. Validação de métodos anal{\'\i}ticos: Como fazer? Por que ela é importante. Bol. Tecnol. e Desenvolv. embalagens 22, 1–9.

Pu, C., Tang, W., 2017. Encapsulation of lycopene in Chlorella pyrenoidosa : Loading properties and stability improvement. Food Chem. 235, 283–289. https://doi.org/10.1016/j.foodchem.2017.05.069

Rahikkala, A., Pereira, S.A.P., Figueiredo, P., Passos, M.L.C., Araújo, A.R.T.S., Saraiva, M.L.M.F.S., Santos, H.A., 2018. Mesoporous Silica Nanoparticles for Targeted and Stimuli-Responsive Delivery of Chemotherapeutics: A Review. Adv. Biosyst. 2, 1–33. https://doi.org/10.1002/adbi.201800020

Rodero, C.F., Fioramonti Calixto, G.M., dos Santos, K., Sato, M.R., dos Santos Ramos, M., Miró, M.S., Rodr\'\iguez, E., Vigezzi, C., Bauab, T.M., Sotomayor, C.E., others, 2018. Curcumin-loaded liquid crystalline systems for controlled drug release and improved treatment of vulvovaginal candidiasis. Mol. Pharm. 15, 4491–4504.

Sábio, R.M., Santagneli, S.H., Gressier, M., Caiut, J.M.A., Pazin, W.M., Ribeiro, S.J.L., Menu, M.-J., 2019. Near-infrared/visible-emitting nanosilica modified with silylated Ru (II) and Ln (III) complexes. Nanotechnology 31, 35602.

Shi, J., Maguer, M. Le, 2000. Lycopene in tomatoes: chemical and physical properties affected by food processing. Crit. Rev. Food Sci. Nutr. 40, 1–42.

SHI, J., MAGUER, M., BRYAN, M., KAKUDA, Y., 2003. KINETICS OF LYCOPENE DEGRADATION IN TOMATO PUREE BY HEAT AND LIGHT IRRADIATION. J. Food Process Eng. 25, 485–498. https://doi.org/10.1111/j.1745-4530.2003.tb00647.x

Tahmasebi, M., Emam-Djomeh, Z., 2021. Lycopene degradation and color characteristics of fresh and processed tomatoes under the different drying methods: a comparative study. Chem. Pap. 75, 3617–3623. https://doi.org/10.1007/s11696-021-01611-0

Takehara, M., Nishimura, M., Kuwa, T., Inoue, Y., Kitamura, C., Kumagai, T., Honda, M., 2014. Characterization and thermal isomerization of (all-E)-lycopene. J. Agric. Food Chem. 62, 264–269.

Tamasi, G., Pardini, A., Croce, R., Consumi, M., Leone, G., Bonechi, C., Rossi, C., Magnani, A., 2021. Combined Experimental and Multivariate Model Approaches for Glycoalkaloid Quantification in Tomatoes. Molecules 26, 3068. https://doi.org/10.3390/molecules26113068

Tsai, S.-Y., Lin, H.-Y., Hong, W.-P., Lin, C.-P., 2017. Evaluation of preliminary causes for vitamin D series degradation via DSC and HPLC analyses. J. Therm. Anal. Calorim. 130, 1357–1369. https://doi.org/10.1007/s10973-017-6209-4

United States Pharmacopeia, 2020a. <1092> The Dissolution Procedure: Development and Validation. 31, 1–11.

United States Pharmacopeia, 2020b. ⟨ 621 ⟩ CHROMATOGRAPHY, 43rd ed. Rockville (USA).

Vaudreuil, M.-A., Vo Duy, S., Munoz, G., Furtos, A., Sauvé, S., 2020. A framework for the analysis of polar anticancer drugs in wastewater: On-line extraction coupled to HILIC or reverse phase LC-MS/MS. Talanta 220, 121407. https://doi.org/10.1016/j.talanta.2020.121407

Vial, J., Jardy, A., 1999. Experimental Comparison of the Different Approaches To Estimate LOD and LOQ of an HPLC Method. Anal. Chem. 71, 2672–2677. https://doi.org/10.1021/ac981179n

Wu, S.-H., Mou, C.-Y., Lin, H.-P., 2013. Synthesis of mesoporous silica nanoparticles. Chem. Soc. Rev. 42, 3862. https://doi.org/10.1039/c3cs35405a

Zhang, Y., Zhi, Z., Jiang, T., Zhang, J., Wang, Z., Wang, S., 2010. Spherical mesoporous silica nanoparticles for loading and release of the poorly water-soluble drug telmisartan. J. Control. Release 145, 257–263. https://doi.org/10.1016/j.jconrel.2010.04.029

Tables

Table 1 is available in the supplementary files section.

Figures

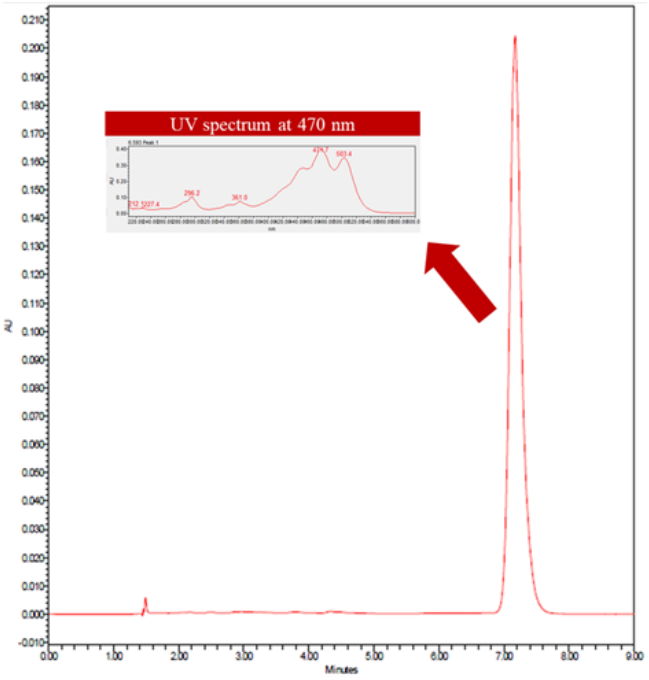

Figure 1

Chromatogram obtained for a 75 µg/mL LYC solution on a C18 column (250 mm × 4.6 mm, 5 µm), maintained at 35 °C with mobile phase of acetonitrile:chloroform (89:11) in an isocratic flow of 2.0 mL min with an injection volume of 20 µL.

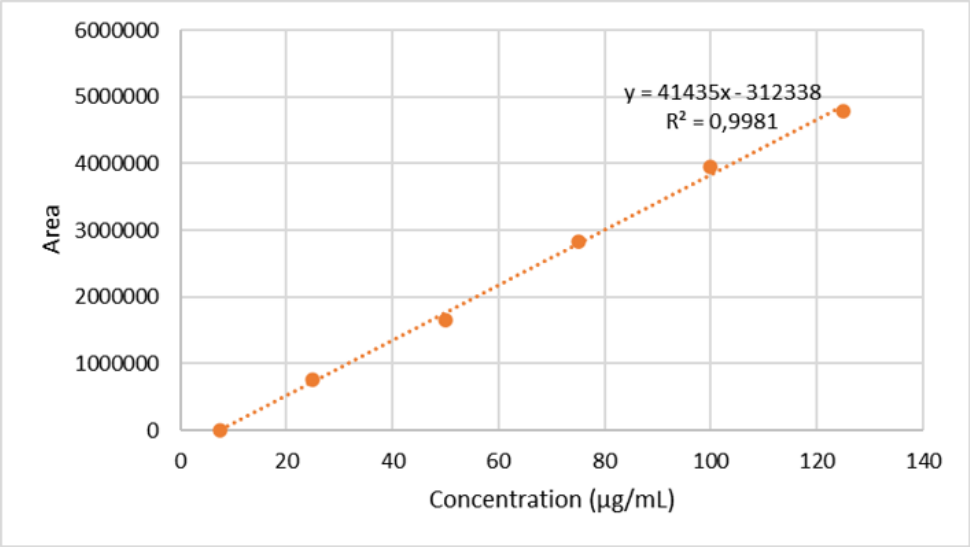

Figure 2

Linear representation of lycopene validation results resulted from the analysis of nine replicates of each concentration by HPLC performed in three different days.

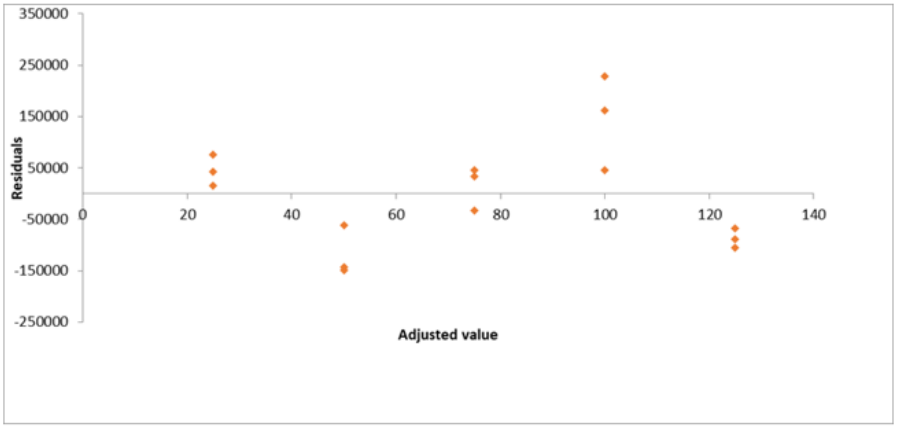

Figure 3

Residual graph of the linear representation of lycopene validation results resulted from the analysis of nine replicates of each concentration by HPLC performed in three different days regression analysis.

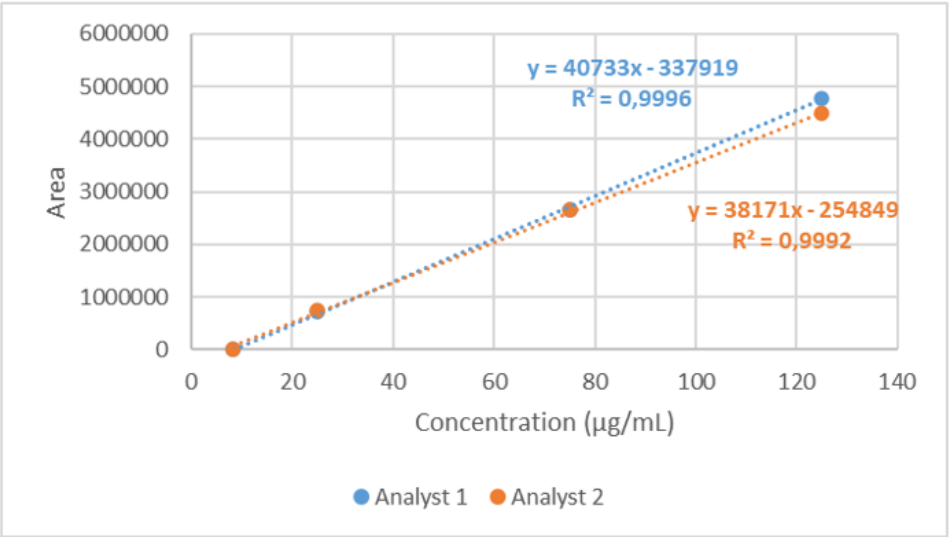

Figure 4

Comparison of the results averages obtained for the intermediate precision of the two analysts performed in triplicate and on different days.

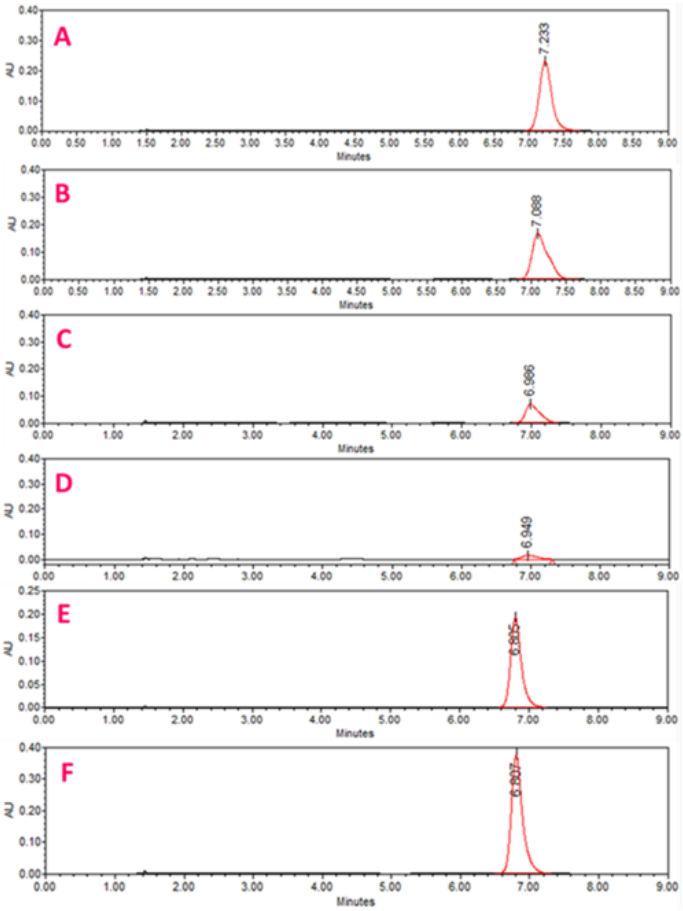

Figure 5

Degradation studies spectra carried out to assess the developed method specificity. Legend: A: standard solution spectrum; B: after temperature degradation; C: after visible light degradation; D: after UV light degradation; E: after changing to pH close to neutral (7.6); F: after changing to basic pH 8.5.

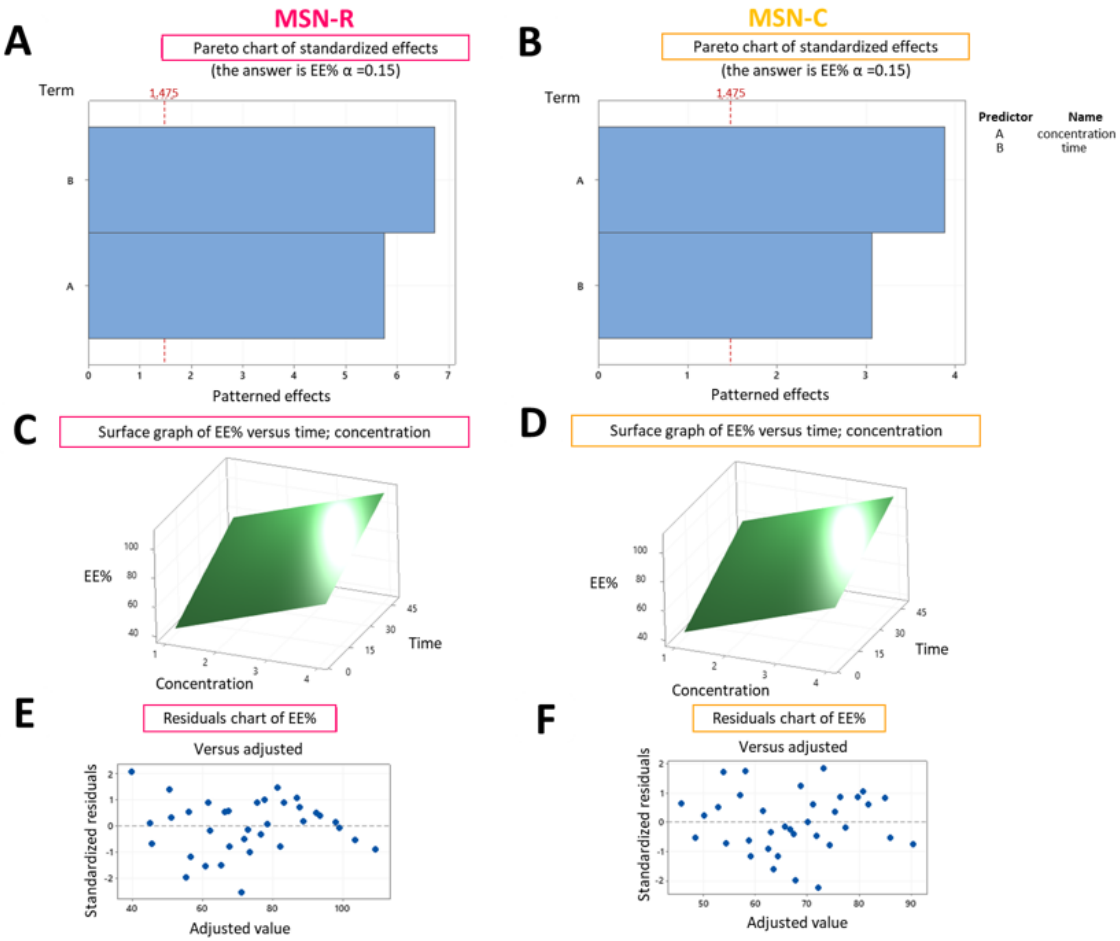

Figure 6

Statistical analysis graphical representation of the time and concentration interference in the EE data from both MSN. (A) Pareto chart of the effect of concentration and time on the EE% of MSN-R. (B) Pareto plot of the effect of concentration and time on the EE% of MSN-C. (C) Surface graph of the effect of concentration and time on the EE% of MSN-R. (D) Surface graph of the effect of concentration and time on the EE% of MSN-C. (E) Pareto analysis residual chart (6A). (F) Pareto analysis residual chart (6B).

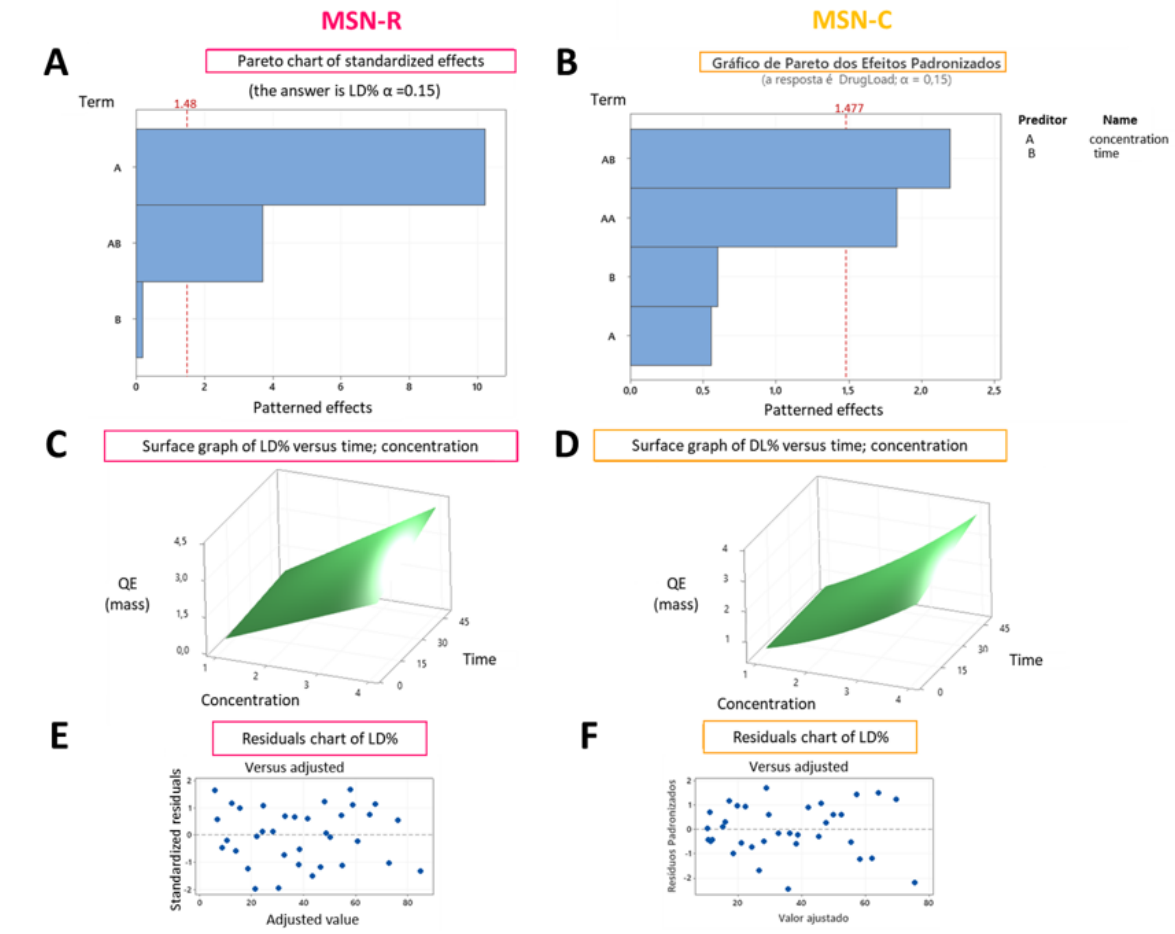

Figure 7

Graphical representation of EE data statistical analysis from both MSN. (A) Pareto chart of the effect of concentration and time on the LD% of MSN-R. (B) Pareto plot of the effect of concentration and time on the LD% of MSN-C. (C) Surface graph of the effect of concentration and time on the LD% of MSN-R. (D) Surface graph of the effect of concentration and time on the LD% of MSN-C. (E) Pareto analysis residual chart (6A). (F) Pareto analysis residual chart (6B).

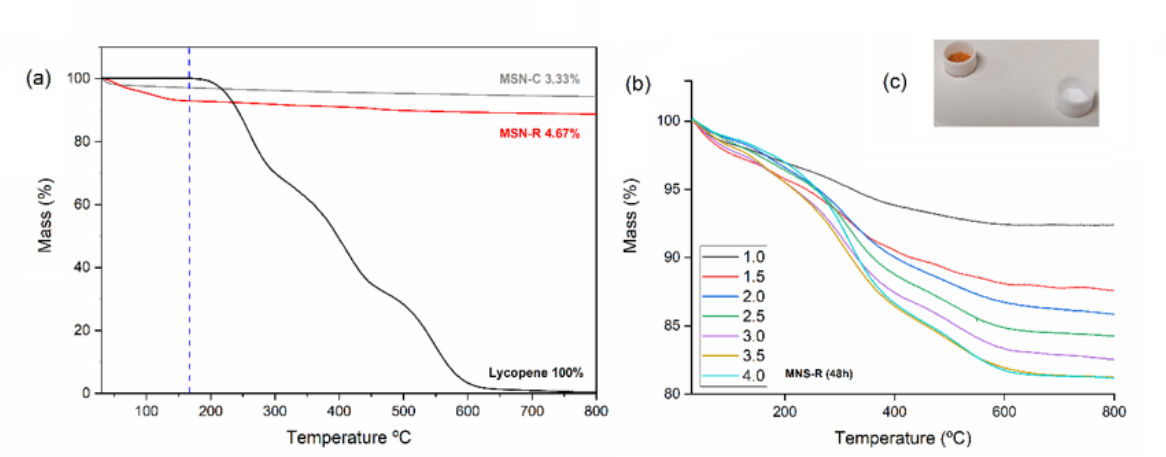

Figure 8

Thermal behavior of LYC, MSN-C, and MSN-R up to 800°C. (A) Thermal behavior of LYC, MSN-C, and MSN-R up to 800°C. (B) MSN-R at 48h incorporated with LYC in different concentrations total mass loss behavior in the TGA curve. (C) incorporated sample before and after the thermal analysis.

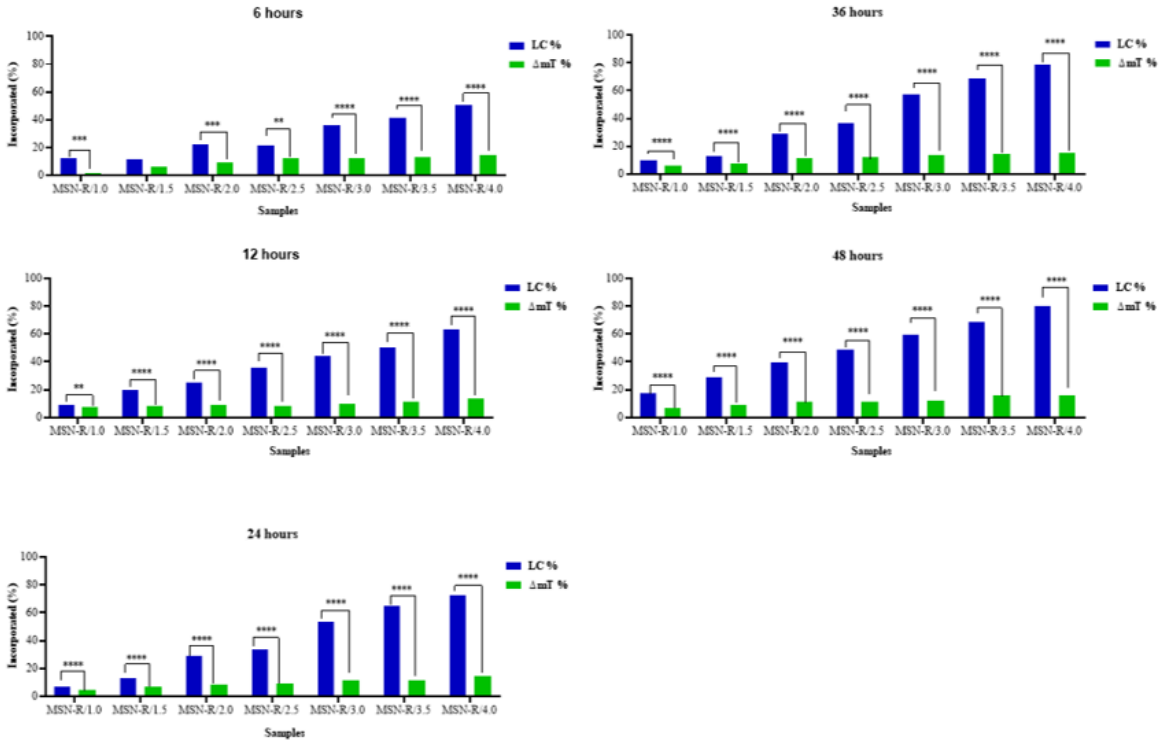

Figure 9

Comparison between Δm_T % and DL% for MSN-R. Legend: p-value; **< 0.005; ***< 0.001; ****<0.0001.

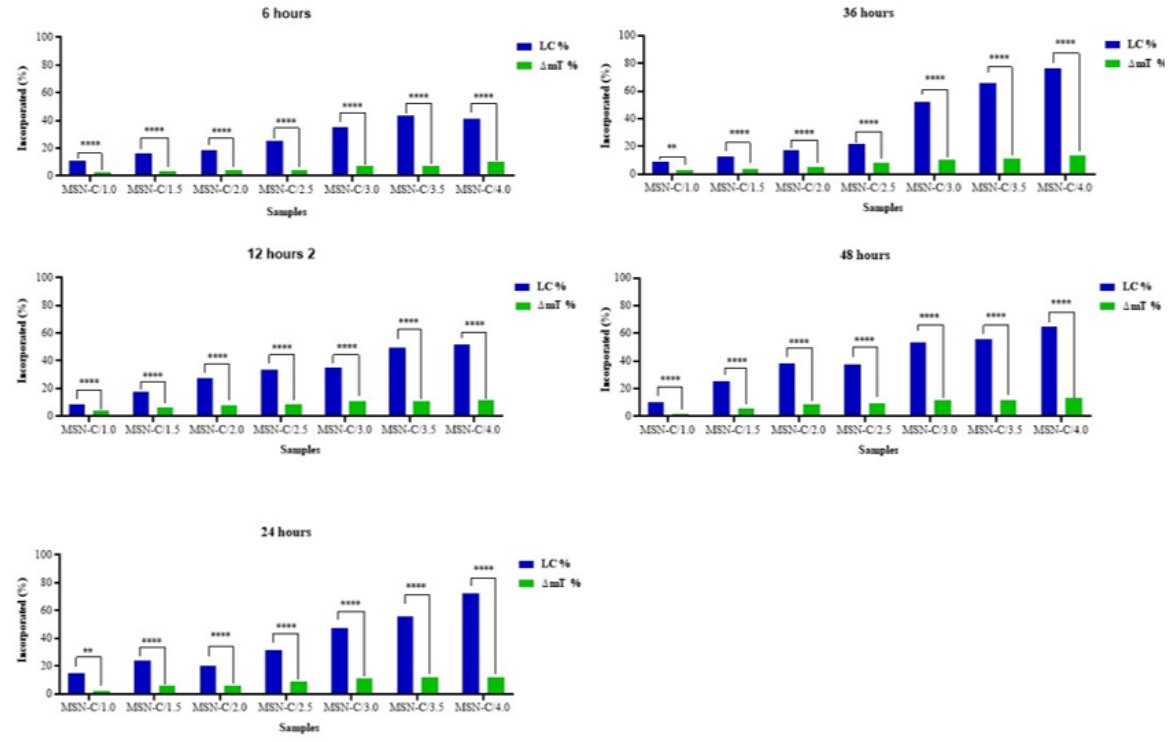

Figure 10

Comparison between Δm_T % and DL% for MSN-C. Legend: p-value; ***<0.001; ****<0.0001.

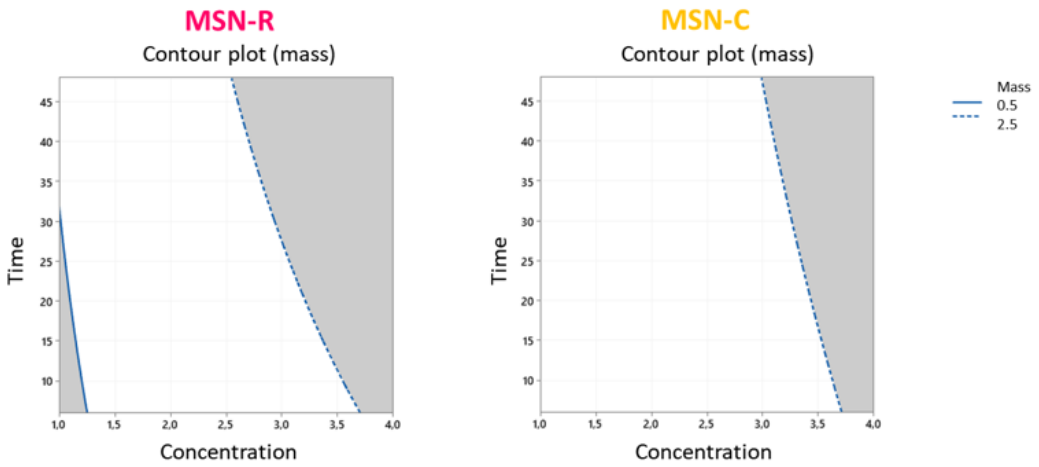

Figure 11

Contour graphic of the conditions tested to incorporate the drug.

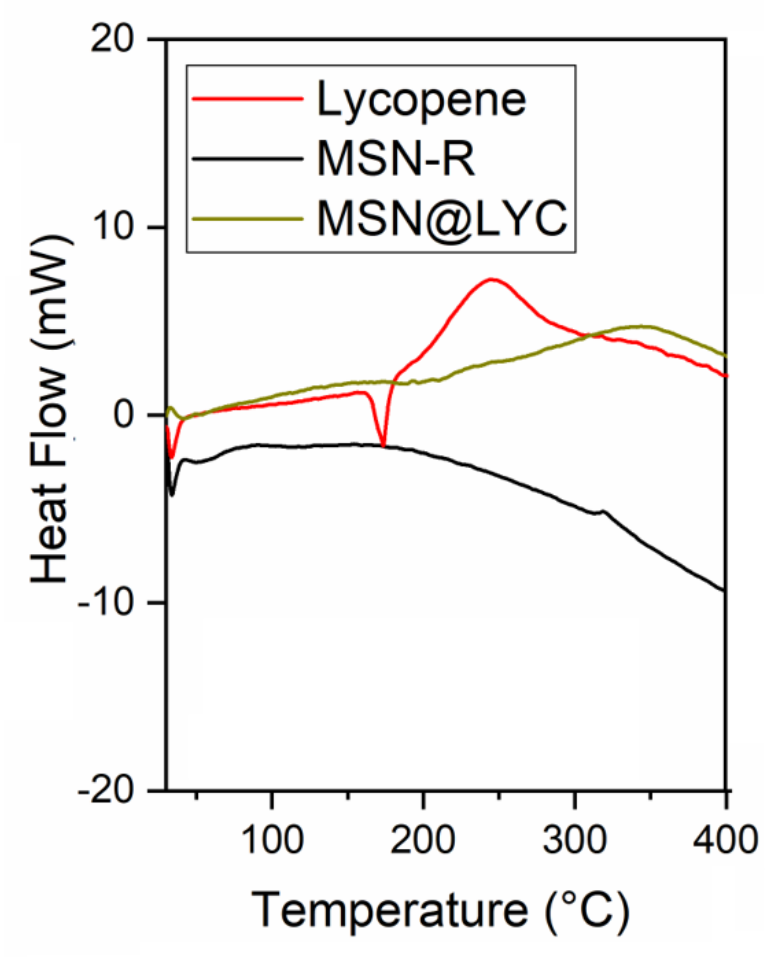

Figure 12

Lycopene, MSN-R and MSN@LYC DSC curves.

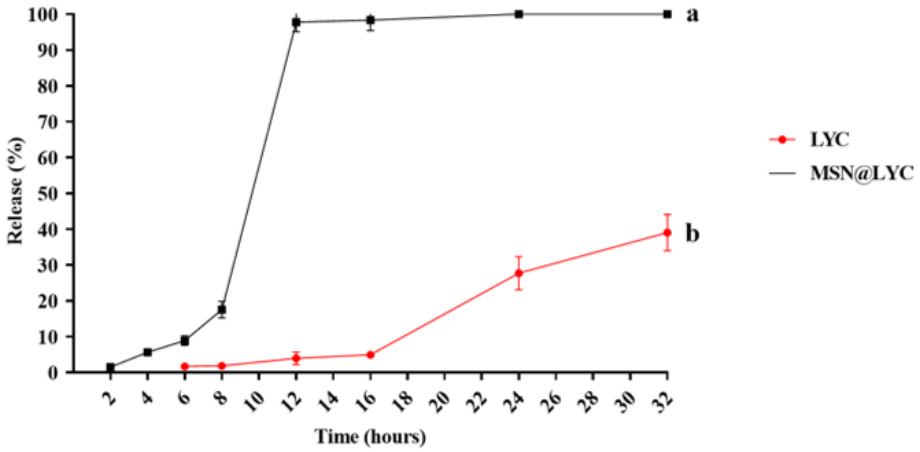

Figure 13

Release profile of MSN@LYC and free lycopene in simulated vaginal medium at a temperature of 37°C under constant agitation of 300 rpm.

Supplementary Files

This is a list of supplementary files associated with this preprint. Click to download.

- APPENDIXA.docx
- GA.jpg
- Table1.docx